EUROPEAN ORGANIZATION FOR NUCLEAR RESEARCH

L3 Note 2552
June 30, 2000

Search for Anomalous ZZγ and Z$\gamma\gamma$ couplings in the process $e^+e^- \rightarrow Z\gamma$ at LEP

The L3 Collaboration

Abstract

We search for anomalous couplings in the ZZγ and Z$\gamma\gamma$ vertices using data collected with the L3 detector at LEP at centre–of–mass energies 192 GeV $\leq \sqrt{s} \leq$ 202 GeV. No evidence is found and preliminary limits are derived from the analysis of the process $e^+e^- \rightarrow Z\gamma$.

Submitted to the *XXXth International Conference on High Energy Physics*
July 27 - August 2, 2000, Osaka, Japan

Introduction

$e^+e^- \to Z\gamma$ is an interesting process to test the existence of new physics [1]. In particular, the existence of anomalous couplings between neutral gauge bosons can be probed by means of this reaction. Effects coming from $ZZ\gamma$ and $Z\gamma\gamma$ couplings are expected to be very small in the Standard Model [1, 2], but can be enhanced in compositeness models [3, 4] or if new particles enter in higher-order corrections.

Assuming only Lorentz and $U(1)_{em}$ gauge invariance, the most general form of the $ZZ\gamma$ and $Z\gamma\gamma$ vertices can be parametrized by means of eight anomalous couplings. The couplings are: h_i^V ($i = 1$ to $4; V = \gamma, Z$), where a V superscript corresponds to a $ZV\gamma$ vertex. The couplings h_1^V and h_2^V are CP violating, whereas h_3^V and h_4^V are CP conserving. The anomalous couplings contribution to the $Z\gamma$ cross section increases with centre–of–mass energy, $\sqrt{s}$, while the Standard Model contribution decreases. All these couplings are zero at tree level in the Standard Model, and only the CP-conserving ones receive a small contribution ($\approx 10^{-4}$) at the one-loop level [1, 2]. An alternative parametrization, which introduces the energy scales of new physics Λ_{iV}, is [5]:

$$\frac{\sqrt{\alpha}\ h_i^V}{m_Z^2} \equiv \frac{1}{\Lambda_{iV}^2}, \quad i = 1, 3 \tag{1}$$

$$\frac{\sqrt{\alpha}\ h_i^V}{m_Z^4} \equiv \frac{1}{\Lambda_{iV}^4}, \quad i = 2, 4. \tag{2}$$

The anomalous couplings h_i^V cannot become arbitrarily large due to unitarity constraints, and should vanish when $s \to \infty$ [6, 7]. For hadron colliders, this means that a form factor dependence should be used [7–10], because the effective centre–of–mass energy of the collision is variable. For e^+e^- colliders, the centre–of–mass energy is fixed and no form factors are needed [11]. Therefore, the results are model independent and no hypothesis about the behaviour close to the new physics scale is made [11, 12]. The main effects of anomalous $ZZ\gamma$ and $Z\gamma\gamma$ couplings are an increase of the $Z\gamma$ total cross section and a modification of the differential spectrum of the photon, mainly at large polar angles. Limits on $ZZ\gamma$ and $Z\gamma\gamma$ couplings have been published at the Tevatron [8–10] and LEP [13, 14].

Data collected by the L3 detector [15] in 1999 at 192 GeV $\leq \sqrt{s} \leq$ 202 GeV amounting to a total luminosity of 230 pb^{-1}, are used to study the anomalous couplings $ZZ\gamma$ and $Z\gamma\gamma$ in the channels $e^+e^- \to q\bar{q}\gamma$ and $e^+e^- \to \nu\bar{\nu}\gamma$.

Event Selection

The main signature of the process $e^+e^- \to Z\gamma$ is the production of a photon of high energy, E_γ. A photon candidate is identified as a shower in the BGO electromagnetic barrel or end-cap calorimeters with more than 90% of its energy deposited in a 3×3 crystal matrix. The mass of the system recoiling against the photon, $m_{rec} = (s - 2E_\gamma\sqrt{s})^{1/2}$, is required to satisfy 80 GeV $< m_{rec} <$ 110 GeV, and thus is consistent with that of a Z. For the $\sqrt{s}$ value considered, the cuts on the recoiling mass correspond to an energy of the photon between 65 GeV and 85 GeV.

In the estimation of signal and background processes the following Monte Carlo generators have been used: KK2F [16] for $e^+e^- \to q\bar{q}\gamma$, $e^+e^- \to q\bar{q}$, KORALZ [17] for $e^+e^- \to \nu\bar{\nu}\gamma$, EXCALIBUR [18] for four-fermion final states, DIAG36 [19] for $e^+e^- \to e^+e^-e^+e^-$, BHWIDE [20]

Process	$\sqrt{s}$ (GeV)	$\mathcal{L}$ (pb^{-1})	ϵ (%)	Events	σ (pb)	σ_{SM} (pb)
$\mathrm{e^+e^-} \rightarrow \mathrm{q\bar{q}}\gamma$	192	29.7	28.2 ± 0.4	101	20.0 ± 2.1	18.8
	196	83.7	27.8 ± 0.2	359	15.7 ± 0.8	17.9
	200	82.8	27.3 ± 0.2	333	18.1 ± 1.1	16.9
	202	37.0	27.4 ± 0.3	163	16.3 ± 1.3	16.3
$\mathrm{e^+e^-} \rightarrow \nu\bar{\nu}\gamma$	192	29.7	29.5 ± 0.7	24	4.5 ± 0.8	4.6
	196	83.7	30.1 ± 0.4	102	4.1 ± 0.4	4.6
	200	82.8	34.6 ± 0.6	96	4.1 ± 0.4	4.5
	202	37.0	31.3 ± 0.5	45	4.0 ± 0.5	4.4

Table 1: The centre–of–mass energies, integrated luminosities, $\mathcal{L}$, and efficiencies, ϵ, of the selection, the number of selected events and the measured cross sectionsi are given for the processes $\mathrm{e^+e^-} \rightarrow \mathrm{q\bar{q}}\gamma$ and $\mathrm{e^+e^-} \rightarrow \nu\bar{\nu}\gamma$. The error on the efficiencies includes the Monte Carlo statistics. The corresponding Standard Model cross sections σ_{SM} [16, 17] are also listed.

and TEEGG [21] for $\mathrm{e^+e^-} \rightarrow \mathrm{e^+e^-}\gamma(\gamma)$. All generated events are passed through a simulation of the L3 detector response [22] and through the same analysis procedure used for data. Time dependent inefficiencies are taken into account in the simulation procedure.

Cross sections and efficiencies are quoted within the following phase space cuts: at least one photon of energy greater than 20 GeV with polar angle in the range $5^\circ < \theta_\gamma < 175^\circ$.

Selection of $\mathrm{e^+e^-} \rightarrow \mathrm{q\bar{q}}\gamma$ events

In addition to a photon candidate recoiling against a Z, high multiplicity and energy-momentum balance are required to select $\mathrm{e^+e^-} \rightarrow \mathrm{q\bar{q}}\gamma$ events:

- The event must have more than 6 tracks and more than 11 calorimetric clusters.
- The transverse energy imbalance must be less than 15% of the visible energy, and the longitudinal energy imbalance less than 20% of the visible energy.
- Events are rejected if the photon candidate has an associated track and $|\cos\theta_\gamma| < 0.9$.
- The polar angle of the photon, θ_γ, must be in the range $|\cos\theta_\gamma| < 0.97$.

The trigger inefficiency is estimated to be negligible due to the redundancy of several triggers for this final state. Two backgrounds are found to contribute: $\mathrm{e^+e^-} \rightarrow \mathrm{q\bar{q}'e}\nu$ and $\mathrm{e^+e^-} \rightarrow \mathrm{q\bar{q}e^+e^-}$, where one of the electrons fakes a photon, giving 0.2% and 0.5% contamination, respectively.

The measured cross sections for $\mathrm{e^+e^-} \rightarrow \mathrm{q\bar{q}}\gamma$ are shown in Table 1 and are in agreement with the Standard Model expectation. Figures 1 and 2 show the recoil mass distribution, the polar angle of the photon and the invariant mass of the $\mathrm{q\bar{q}}$ system.

Selection of $\mathrm{e^+e^-} \rightarrow \nu\bar{\nu}\gamma$ events

In addition to the presence of a photon, the selection criteria for the $\mathrm{e^+e^-} \rightarrow \nu\bar{\nu}\gamma$ channel require low activity in the detector and large energy-momentum imbalance.

- The event cannot have more than 10 calorimetric clusters. The number of hits in the tracking chamber associated with a calorimetric cluster must not exceed 40% of the expected number of hits for a charged track.
- The polar angle of the photon candidate must satisfy $|\cos\theta_\gamma| < 0.96$.
- The transverse and total energy imbalances in the event must be greater than 20% and 95% of the visible energy, respectively.
- To suppress cosmic ray background, there must be at least one scintillator time measurement within ± 5 ns of the beam crossing time. The scintillator signals must be associated with calorimetric clusters.

The trigger efficiency is estimated to be 96%, using an independent sample of data events. The background in the selected sample is found to be negligible. The measured cross sections for $\mathrm{e^+e^-} \rightarrow \nu\bar{\nu}\gamma$ are shown in Table 1. They are in agreement with the Standard Model expectations. Figure 3 shows the recoil mass distribution and Figure 4 gives the polar angle distribution of the photon.

Results

The analysis is performed by means of the "Optimal Variables" [23] approach. The differential cross section of the process $\mathrm{e^+e^-} \rightarrow \mathrm{Z}\gamma$ is written as a function of the anomalous couplings:

$$\frac{d\sigma}{d\vec{\Omega}} = c_0(\vec{\Omega}) + \sum_{i=1}^{4} \sum_{V=\gamma,\mathrm{Z}} c_{1,i,V}(\vec{\Omega}) h_i^V + \sum_{i=1}^{4} \sum_{V=\gamma,\mathrm{Z}} \sum_{j=1}^{4} \sum_{V'=\gamma,\mathrm{Z}} c_{2,ij,V,V'}(\vec{\Omega}) h_i^V h_j^{V'}, \tag{3}$$

where c_0, $c_{1,i,V}$ and $c_{2,ij,V,V'}$ are function of $\vec{\Omega} = (E_\gamma, \theta_\gamma, \phi_\gamma, \theta_f^{\mathrm{Z}}, \phi_f^{\mathrm{Z}})$. Here, E_γ, θ_γ and ϕ_γ are the energy and angular variables of the photon, and $\theta_f^{\mathrm{Z}}, \phi_f^{\mathrm{Z}}$ the angles of the fermion f in the Z rest frame. For the $\mathrm{e^+e^-} \rightarrow \nu\bar{\nu}\gamma$ case, the neutrino angular variables are integrated out, leaving three variables in the calculation. As the couplings are small, the quadratic term is neglected, and the optimal variable for each coupling is defined as:

$$\mathcal{O}_{1,i,V} \equiv \frac{c_{1,i,V}(\vec{\Omega})}{c_0(\vec{\Omega})}. \tag{4}$$

This method profits from having a one-dimensional parametrization which uses all the available kinematic information.

A binned maximum likelihood fit of the expected optimal variable distribution to the data is performed. A reweighting technique is used to compute the expected number of events in the presence of anomalous couplings. In these fits, only one coupling is fitted each time, keeping all the other couplings at zero. The distributions of the optimal variables for the couplings h_1^{Z} and h_4^γ are shown as an example in Figures 5 and 6, respectively.

No deviations from the Standard Model expectations are found. Both the $\mathrm{q\bar{q}}\gamma$ and $\nu\bar{\nu}\gamma$ samples lead to the same results. The limits on the anomalous couplings at 95% confidence level (CL) found from combining the samples are:

$$
\begin{array}{ll}
-0.16 < h_1^{\mathrm{Z}} < 0.07 & -0.16 < h_1^{\gamma} < 0.05 \\
-0.05 < h_2^{\mathrm{Z}} < 0.10 & -0.04 < h_2^{\gamma} < 0.09 \\
-0.19 < h_3^{\mathrm{Z}} < 0.13 & -0.12 < h_3^{\gamma} < 0.00 \\
-0.07 < h_4^{\mathrm{Z}} < 0.12 & -0.00 < h_4^{\gamma} < 0.08.
\end{array}
$$

Figure 7 shows the comparison between these results and the results obtained using the data collected by L3 in 1998 [13]. The higher centre-of-mass energy allows an increase of the sensitivity to the anomalous couplings.

Fits to the two-dimensional distributions of the optimal observables are performed to determine the pairs of CP-violating and CP-conserving couplings, keeping in each case all other couplings fixed at zero. Results at 95% CL are shown in Figures 8 and 9.

If the data are interpreted in terms of new physics scales using formulae (1) and (2), the following lower limits (95% CL) are obtained:

$$
\begin{array}{ll}
\Lambda_{1\mathrm{Z}} > 1030 \text{ GeV} & \Lambda_{1\gamma} > 1165 \text{ GeV} \\
\Lambda_{2\mathrm{Z}} > 304 \text{ GeV} & \Lambda_{2\gamma} > 306 \text{ GeV} \\
\Lambda_{3\mathrm{Z}} > 809 \text{ GeV} & \Lambda_{3\gamma} > 1674 \text{ GeV} \\
\Lambda_{4\mathrm{Z}} > 293 \text{ GeV} & \Lambda_{4\gamma} > 331 \text{ GeV}.
\end{array}
$$

To obtain these results, the maximum of the likelihood is taken as the Standard Model expectation. To determine the confidence levels, the probability distributions are normalized over the physically allowed range of the parameters.

References

[1] F.M. Renard, Nucl. Phys. **B 196** (1982) 93.

[2] A. Barroso *et al.*, Z. Phys. **C 28** (1985) 149.

[3] F.M. Renard, Phys. Lett. **B 126** (1983) 59.

[4] M. Claudson, E. Farhi and R.L. Jaffe, Phys. Rev. **D 34** (1986) 873.

[5] P. Mery, M. Perrotet and F.M. Renard, Z. Phys. **C 38** (1988) 579.

[6] H. Czyz, K. Kołodziej and M. Krałek, Z. Phys. **C 43** (1989) 97.

[7] U. Baur and E. Berger, Phys. Rev. **D 47** (1993) 4889.

[8] CDF Collab., F. Abe *et al.*, Phys. Rev. Lett. **74** (1995) 1941.

[9] D0 Collab., S. Abachi *et al.*, Phys. Rev. Lett. **78** (1997) 3640.

[10] D0 Collab., B. Abbott *et al.*, Phys. Rev. **D 57** (1998) 3817.

[11] G. J. Gounaris, J. Layssac and F. M. Renard, Phys. Rev. **D 61** (2000) 073013.

[12] J. Wudka, hep-ph/9606478, *The meaning of anomalous couplings*, in Physics and Technology of the Next Linear Collider; eds. D. Burke and M. Peskin.

[13] L3 Collab., M. Acciarri *et al.*, Submitted to Phys. Lett. **B** (2000).

[14] DELPHI Collab., P. Abreu *et al.*, Phys. Lett. **B 423** (1998) 194.

[15] L3 Collab., B. Adeva *et al.*, Nucl. Inst. and Meth. **A289** (1990) 35;
L3 Collab., M. Chemarin *et al.*, Nucl. Inst. and Meth. **A349** (1994) 345;
L3 Collab., M. Acciarri *et al.*, Nucl. Inst. and Meth. **A351** (1994) 300;
L3 Collab., A. Adam *et al.*, Nucl. Inst. and Meth. **A383** (1996) 342.

[16] S. Jadach *et al.*, hep-ph/9912214, Comp. Phys. Comm. accepted.

[17] S. Jadach, B.F.L. Ward and Z. Wąs, Comp. Phys. Comm **79** (1994) 503.

[18] F.A. Berends, R. Kleiss and R. Pittau, Nucl. Phys. **B 424** (1994) 308; Nucl. Phys. **B 426** (1994) 344; Nucl. Phys. (Proc. Suppl.) **B 37** (1994) 163;
R. Kleiss and R. Pittau, Comp. Phys. Comm. **85** (1995) 447;
R. Pittau, Phys. Lett. **B 335** (1994) 490.

[19] F.A. Berends, P.H. Daverfelt and R. Kleiss, Nucl. Phys. **B 253** (1985) 441;
Comp. Phys. Comm. **40** (1986) 285.

[20] S. Jadach, W. Placzek and B.F.L. Ward, hep-ph/9608412;
S. Jadach *et al.*, 'Event Generators for Bhabha Scattering',
in 'Physics at LEP2', eds. G. Altarelli, T. Sjostrand, F. Zwirner,
(CERN, Geneva, 1996), Yellow Report CERN 96-01, Vol. 2, p. 229,
hep-ph/9602393.

[21] D. Karlen, Nucl. Phys. **B 289** (1987) 23.

[22] The L3 detector simulation is based on GEANT Version 3.15.
R. Brun *et al.*, "GEANT 3", CERN–DD/EE/84–1 (Revised), 1987.
The GHEISHA program (H. Fesefeldt, RWTH Aachen Report PITHA 85/02 (1985)) is used to simulate hadronic interactions.

[23] M. Diehl and O. Nachtmann, Z. Phys. **C 62** (1994) 397.

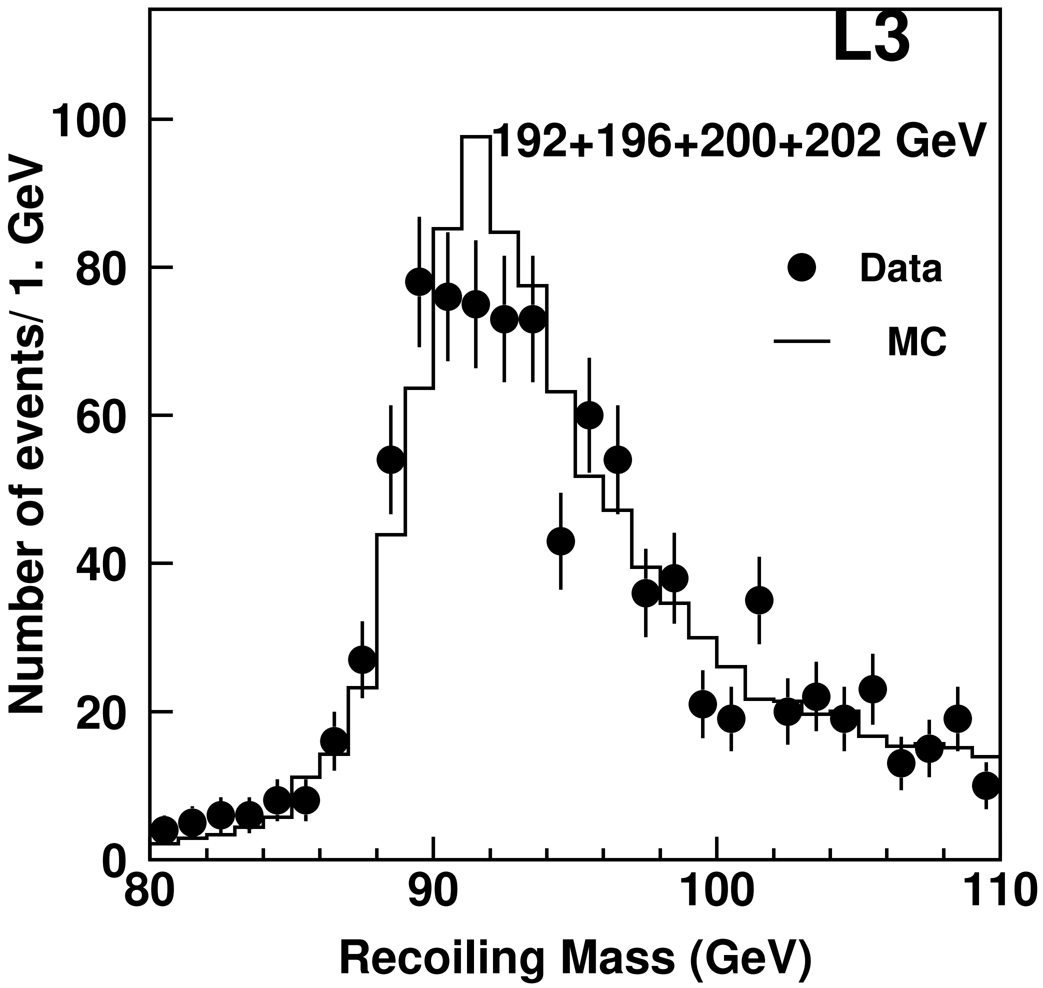

Figure 1: Distribution of the mass recoiling from the photon candidate in $e^+e^- \rightarrow q\bar{q}\gamma$ events. The points are data and the histogram is the Standard Model Monte Carlo prediction.

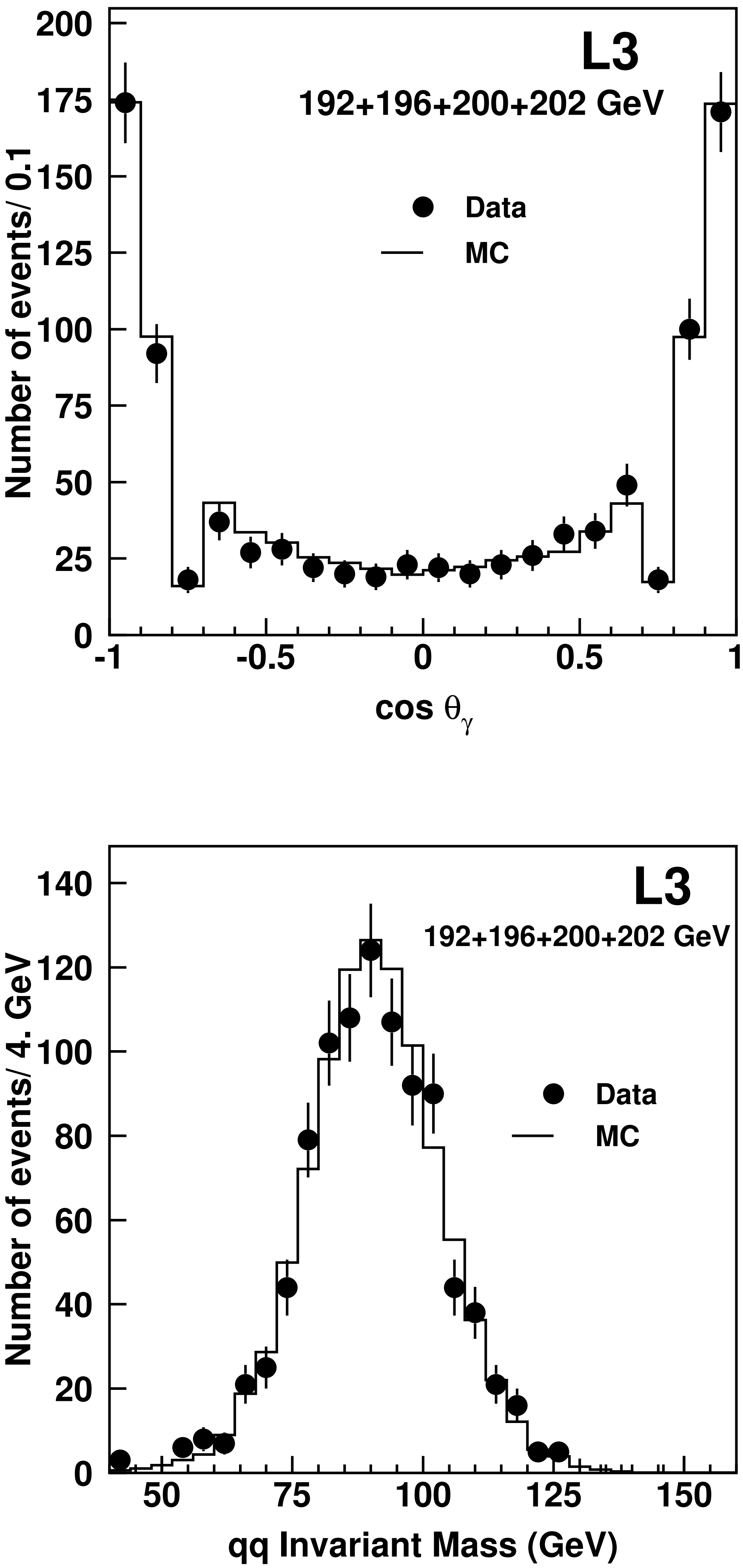

Figure 2: Polar angle of the photon and invariant mass of the $q\bar{q}$ system distributions in $e^+e^- \rightarrow q\bar{q}\gamma$ events. The points are data and the histogram is the Standard Model Monte Carlo prediction.

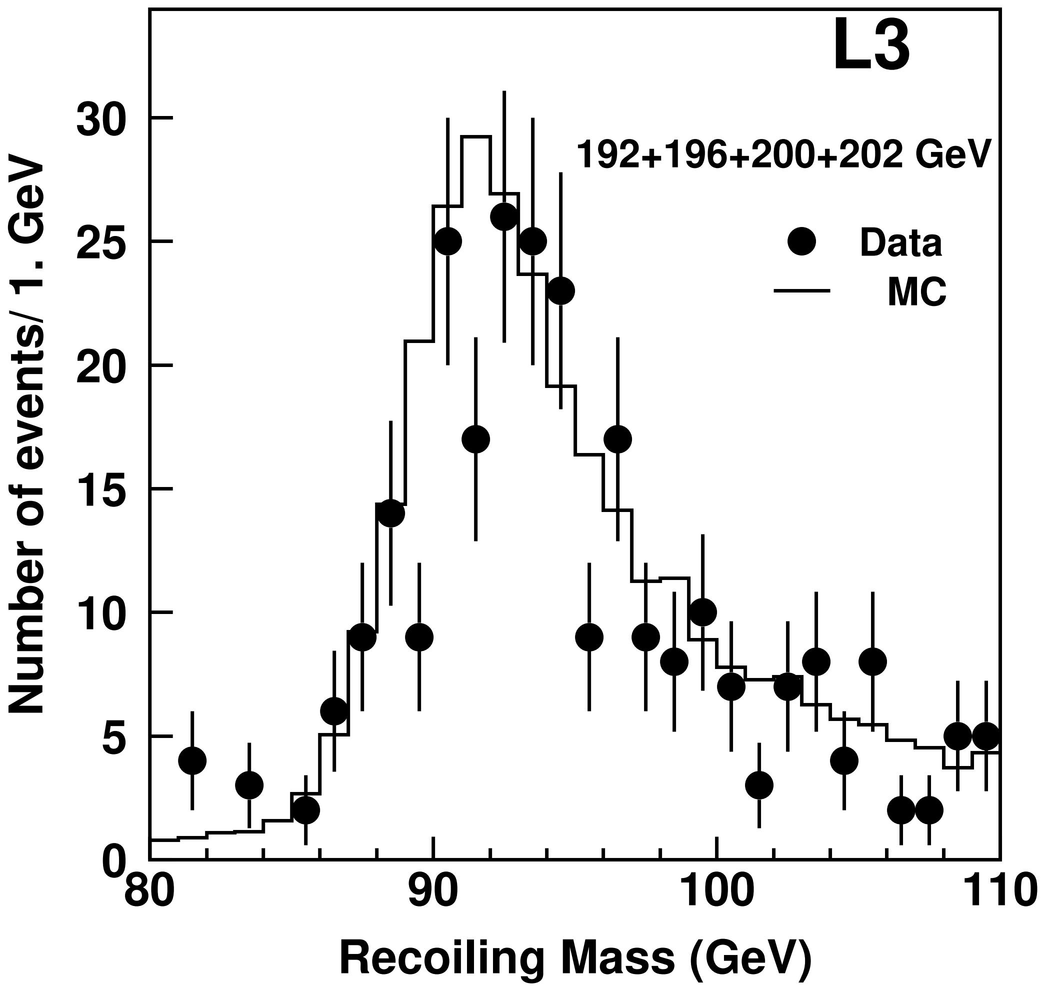

Figure 3: Distribution of the mass recoiling from the photon candidate in $e^+e^- \rightarrow \nu\bar{\nu}\gamma$ events. The points are data and the histogram is the Standard Model Monte Carlo prediction.

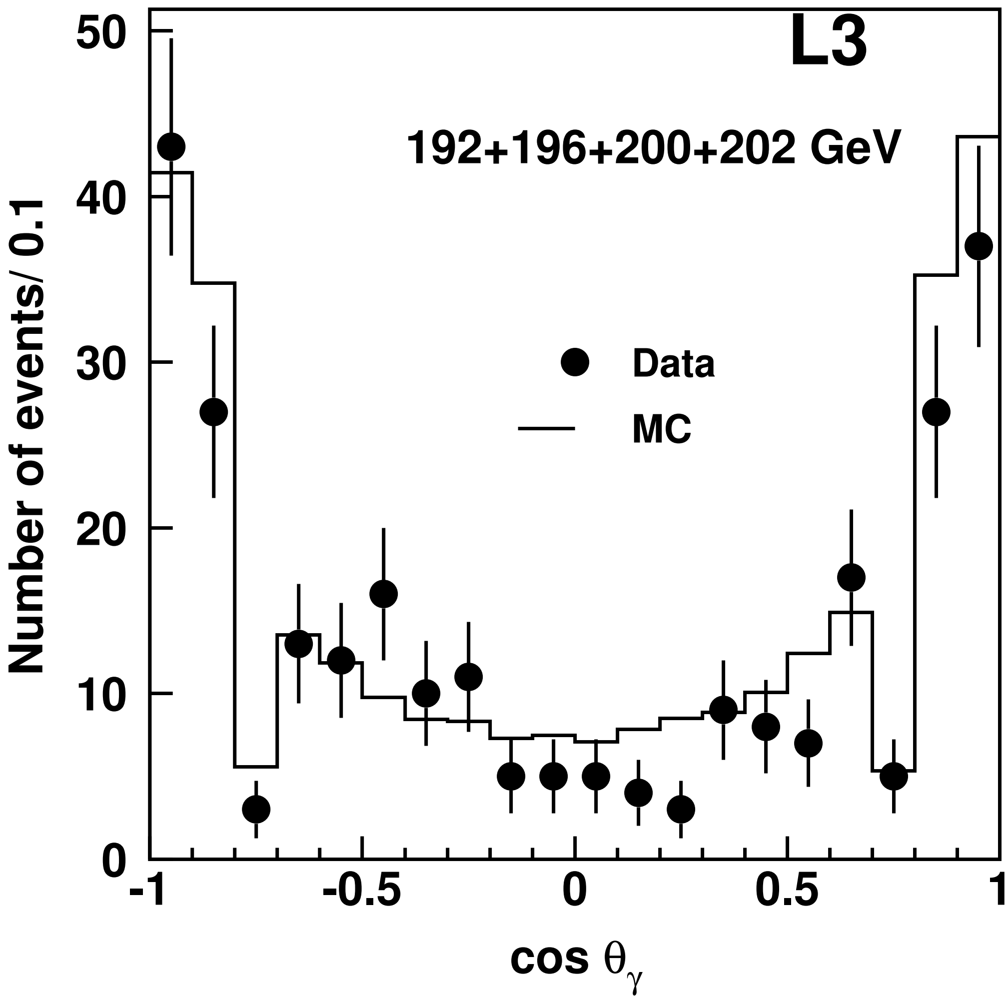

Figure 4: Polar angle distribution from the photon candidates in $e^+e^- \rightarrow \nu\bar{\nu}\gamma$ events. The points are data and the histogram is the Standard Model Monte Carlo prediction.

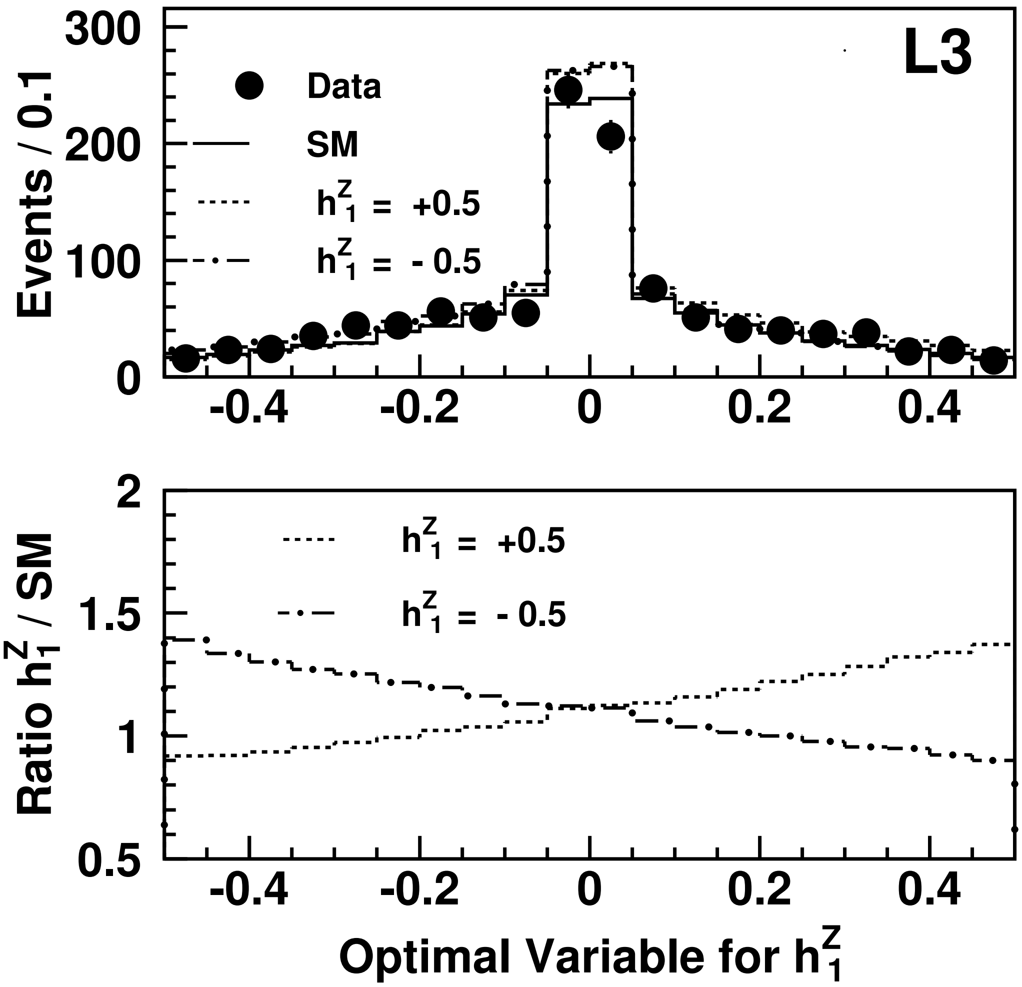

Figure 5: Distribution of the optimal variable for the CP violating coupling h_1^Z. Data are shown, together with the expectations for the Standard Model (SM) and for anomalous couplings, $h_1^Z = \pm 0.5$. In the lower plot the ratio between the anomalous couplings contribution, $h_1^Z = \pm 0.5$, and the SM expectation is presented.

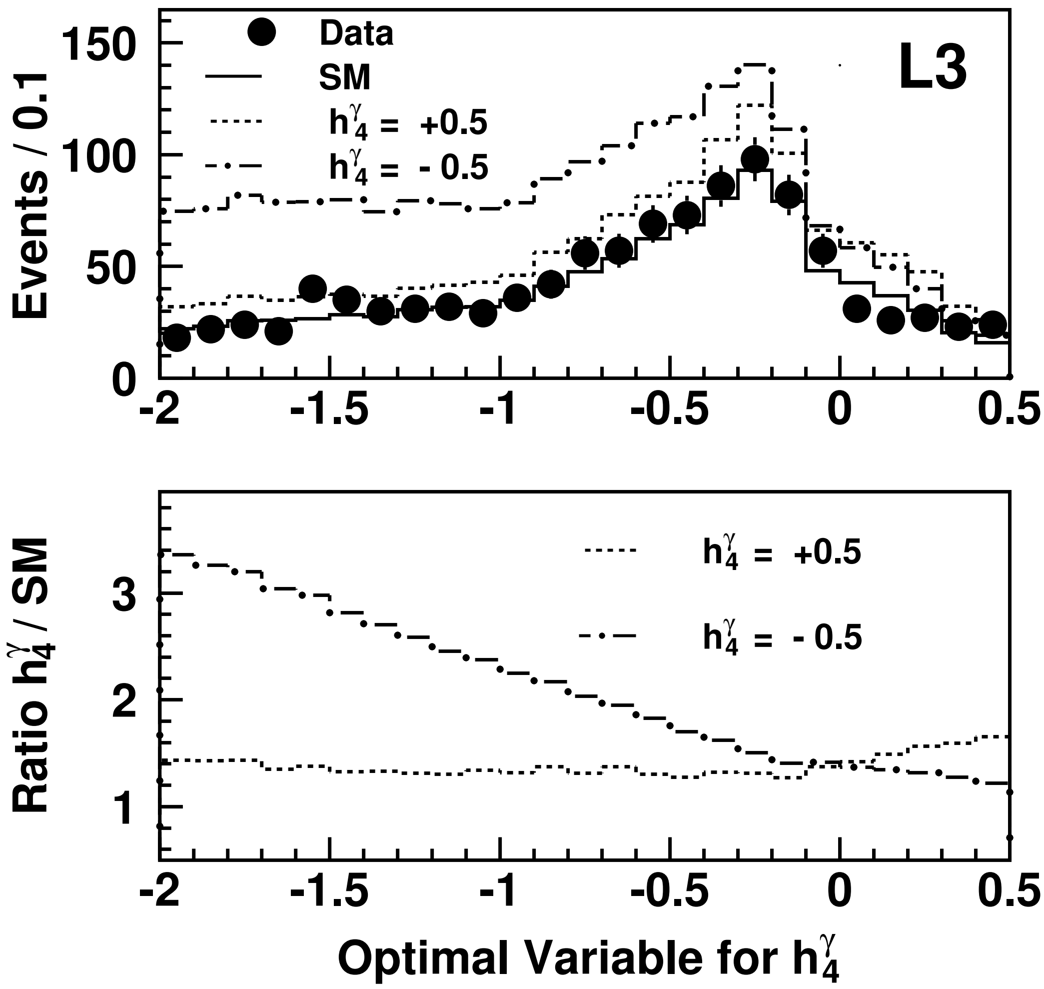

Figure 6: Distribution of the optimal variable for the CP conserving coupling h_4^γ. Data are shown, together with the expectations for the Standard Model (SM) and for anomalous couplings, $h_4^\gamma = \pm 0.5$. In the lower plot the ratio between the anomalous couplings contribution, $h_4^\gamma = \pm 0.5$, and the SM expectation is presented.

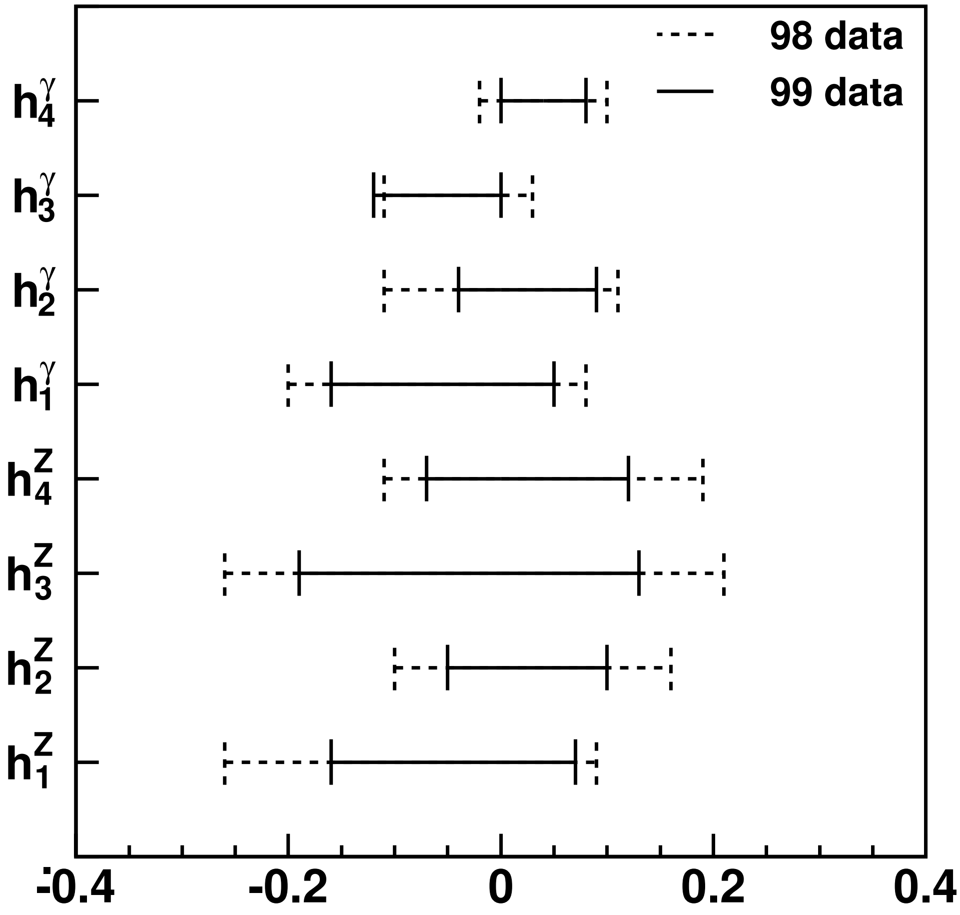

Figure 7: Comparison between the 95% CL limits on anomalous couplings obtained using the L3 1998 [13] and 1999 data samples.

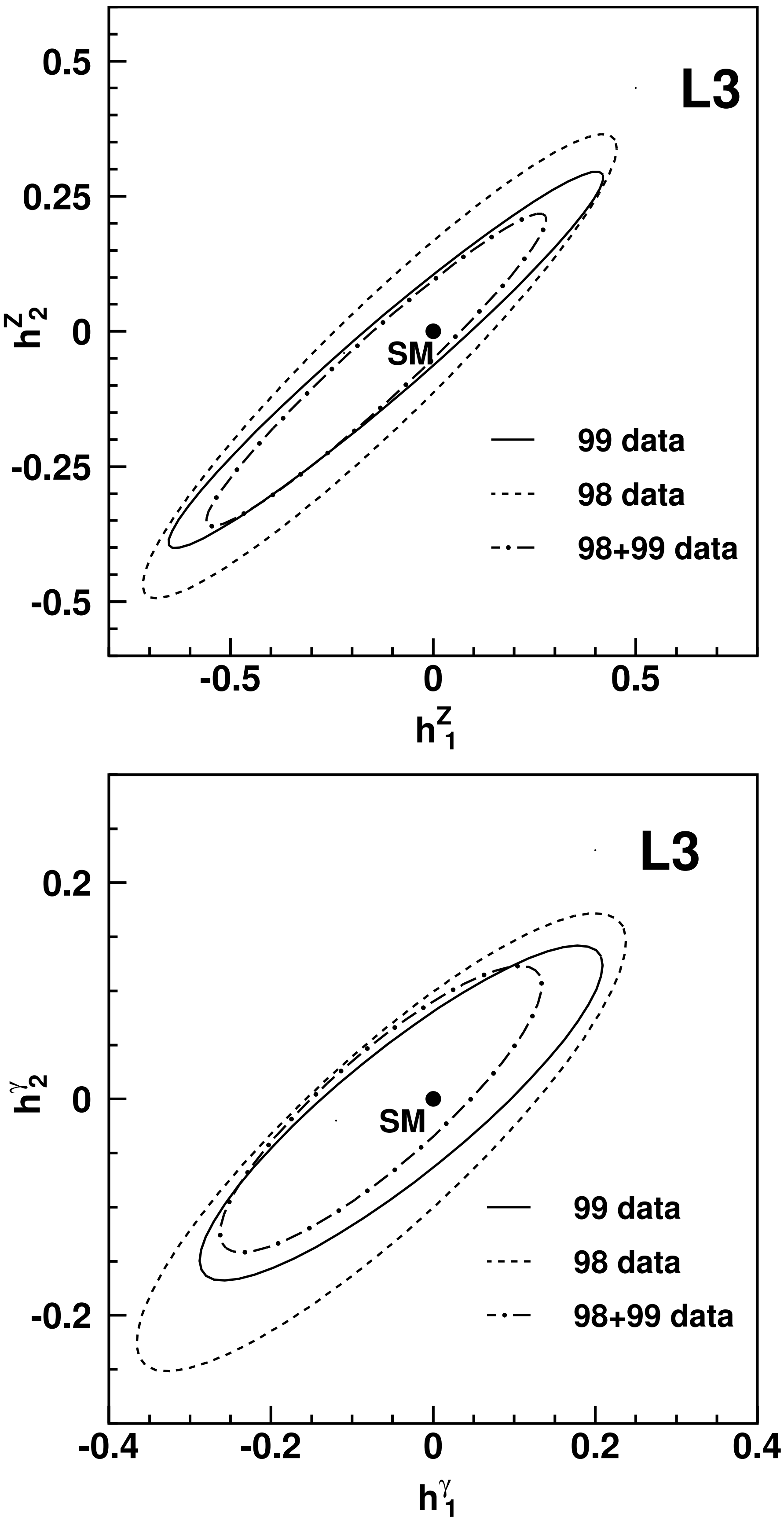

Figure 8: Limits at 95% CL on the CP-violating coupling parameters, h_2^Z versus h_1^Z and h_2^γ versus h_1^γ. The Standard Model predictions are indicated by the points. The regions outside the contours are excluded. Results using the 1998 data sample [13] and the combination of both are also shown for comparison.

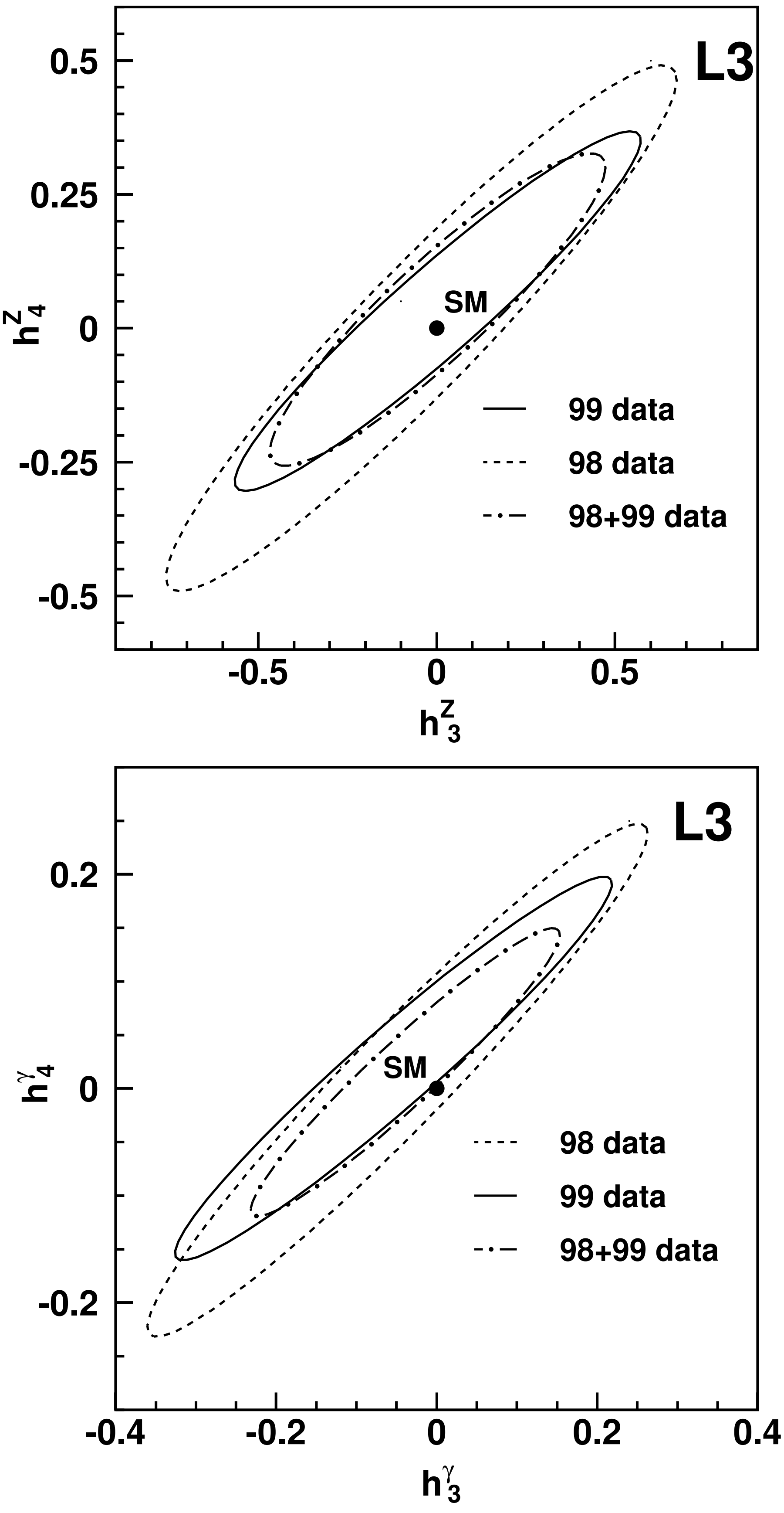

Figure 9: Limits at 95% CL on the CP-conserving coupling parameters, h_4^Z versus h_3^Z and h_4^γ versus h_3^γ. The Standard Model predictions are indicated by the points. The regions outside the contours are excluded. Results using the 1998 data sample [13] and the combination of both are also shown for comparison.